Science Advances

AAAS

Supplementary Materials for

Microglia response following acute demyelination is heterogeneous and limits infiltrating macrophage dispersion

Jason R. Plemel*, Jo Anne Stratton, Nathan J. Michaels, Khalil S. Rawji, Eric Zhang, Sarthak Sinha, Charbel S. Baaklini,
Yifei Dong, Madelene Ho, Kevin Thorburn, Timothy N. Friedman, Sana Jawad, Claudia Silva, Andrew V. Caprariello,
Vahid Hoghooghi, Julie Yue, Arzina Jaffer, Kelly Lee, Bradley J. Kerr, Raj Midha,
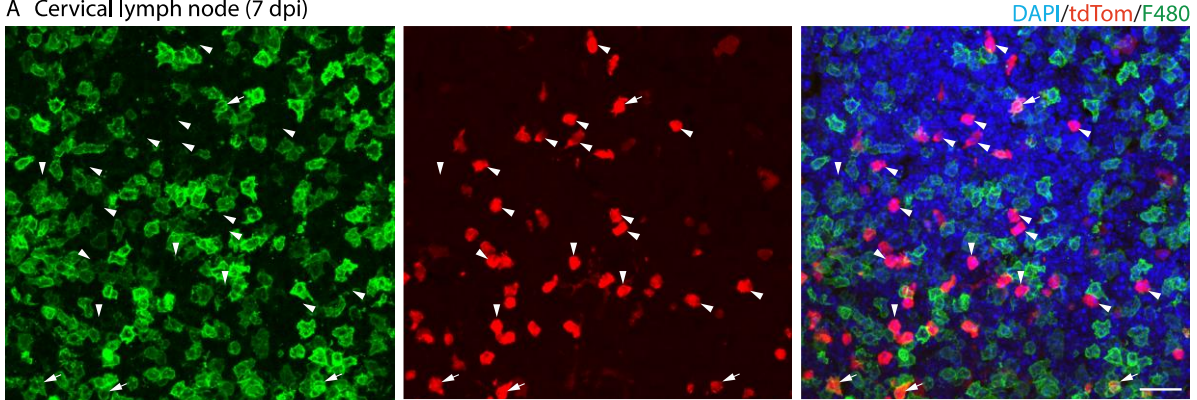Peter K. Stys, Jeff Biernaskie*, V. Wee Yong*

*Corresponding author. Email: jrplemel@ualberta.ca (J.R.P.); jabierna@ucalgary.ca (J.B.);
vyong@ucalgary.ca (V.W.Y.)

This PDF file includes:

A Cervical lymph node (7 dpi)

DAPI/tdTom/F480

B Spleen (7 dpi)

DAPI/tdTom/F480

Fig. S1. Minimal expression of Cx3Cr1^{creER}-TdTom in monocytes or macrophages in the spleen and lymph node. TdTom+ cells were present in the spleen and lymph node. Importantly, only 3-5% of these cells were monocytes or macrophages (arrows) as evidenced by a lack of F4/80 immunocytochemical staining in the majority of TdTom+ cells (arrowheads;(*65*)). Scale bar, 20 μm.
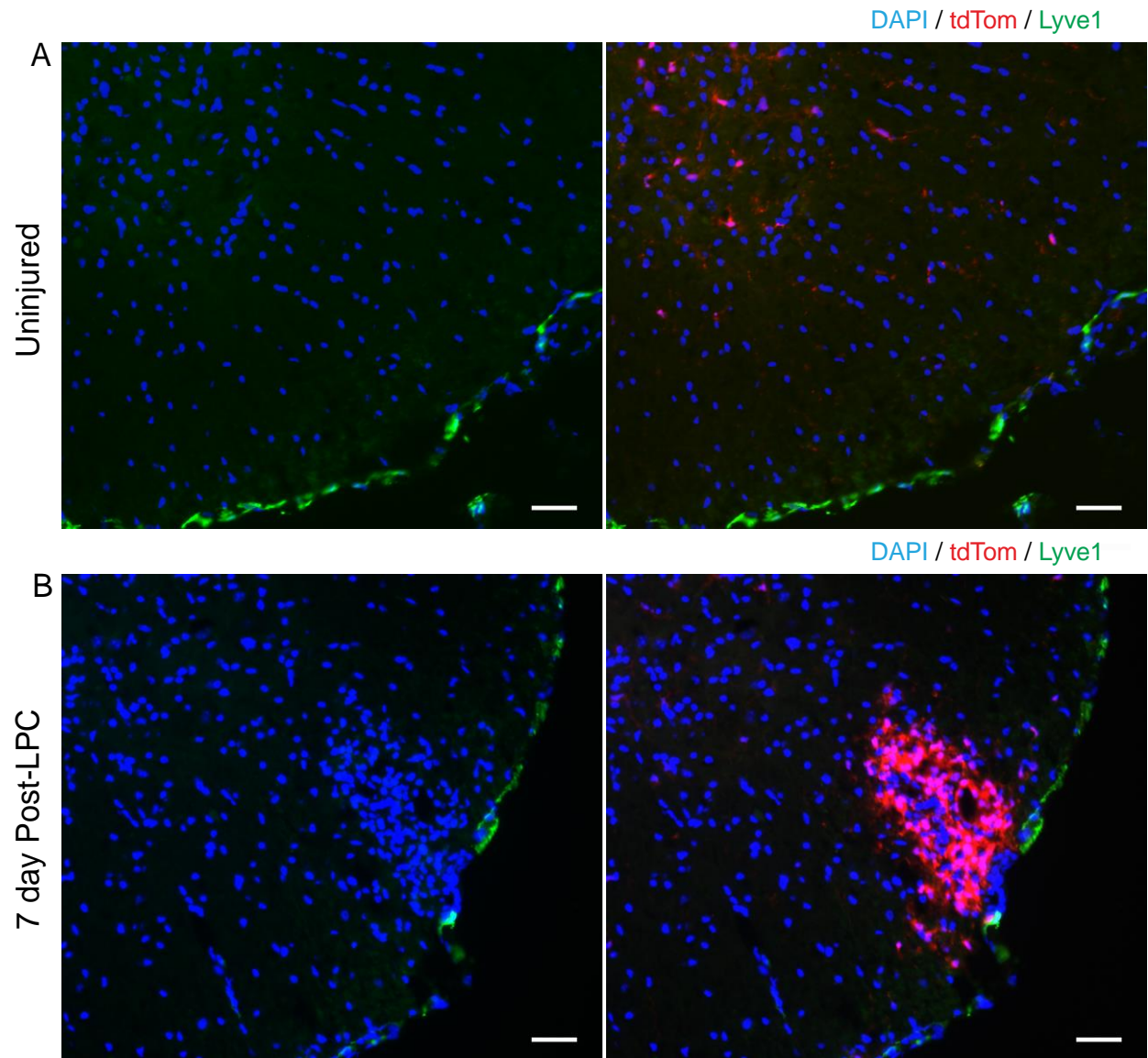
Fig. S2. Lack of meningeal or perivascular macrophage marker Lyve1. In the uninjured spinal cord, the expression of Lyve1 is on cells that line the spinal cord meninges (**A**). After LPC mediated demyelination there was an expansion of tdTom⁺ fate mapped microglia, which did not express Lyve1 (**B**). Lyve+ cells are not found in the lesion delineated by the hypercellularity. Scale bar, 20 μm.
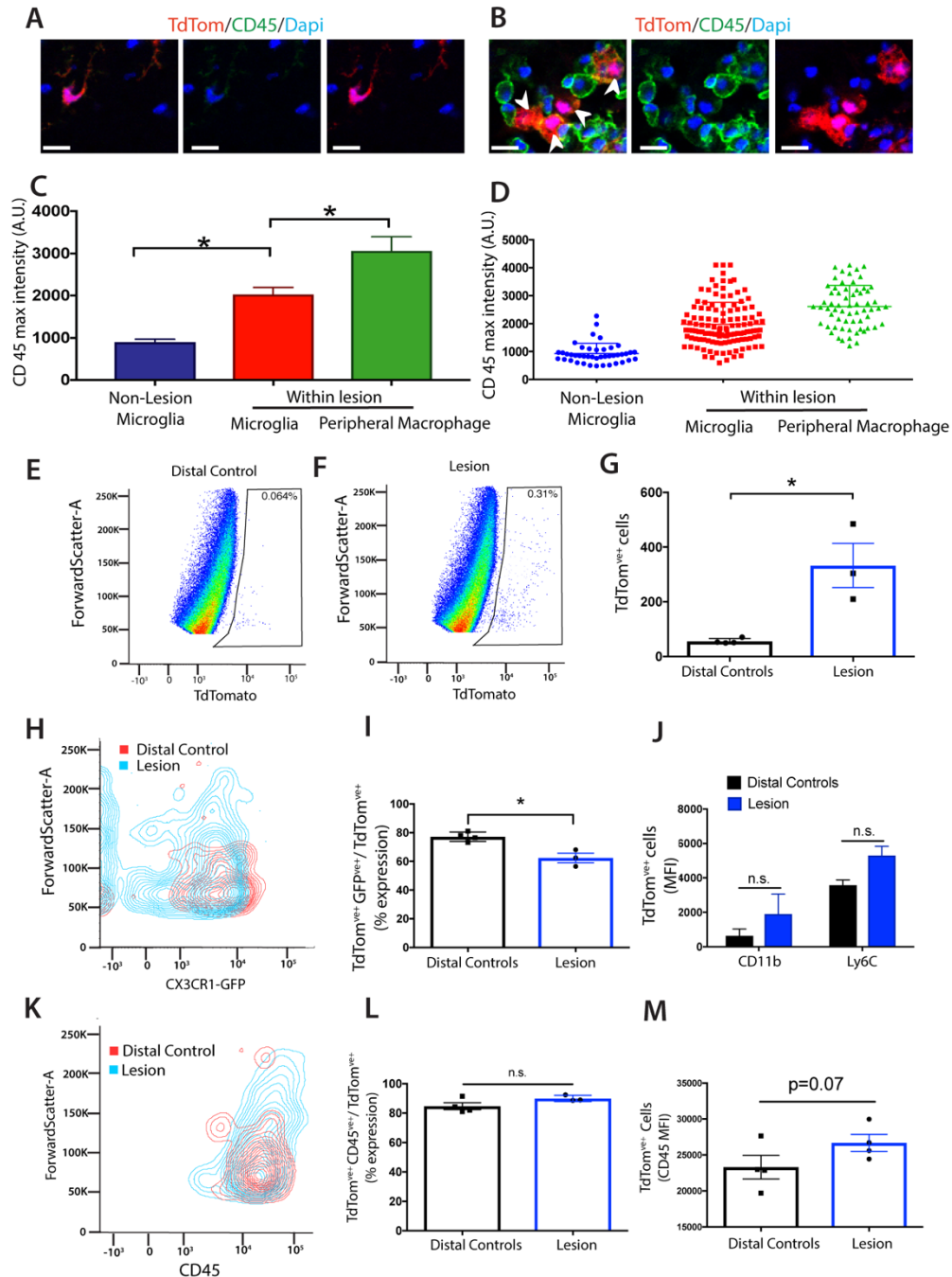
**Fig. S3. Common markers to distinguish microglia and macrophages are less sensitive after microglia activation.** (**A, B**) Representative immunohistochemical images of the uninjured (A) and injured (B) spinal cord demonstrating the expression of CD45 (B, green) in tdTom positive cells (red). This observation was also reflected in quantification (**C, D**). (**E-G**) Representative flow cytometry plots (E, F) and flow quantification (G) of reporter expression demonstrating an increase in tdTom+ expression after injury in the spinal cords of injured mice at 7 days post-LPC. (**H-M**) Representative flow cytometry plots (H, K) and flow quantification (I, J, L, M) of tdTom+ cells, expressing either CX3CR1-EYFP, CD45, CD11b or Ly6C. There was a decrease in tdTom+ cells expressing CX3CR1-EYFP (H, I) but no difference in the mean fluorescent

intensity (MFI) of cells expressing CD11b or Ly6C (J). In addition, there was a trend towards dTom+ cells expressing high levels of CD45 (K-M). n = 4 (B, D), n=3-4 (G, I, J, L, M); (A) ANOVA with Tukey's multiple comparison test or (G, I, J, L, M) Unpaired T-test; Error bars indicate ± SEM. Scale bar, 10 μm.
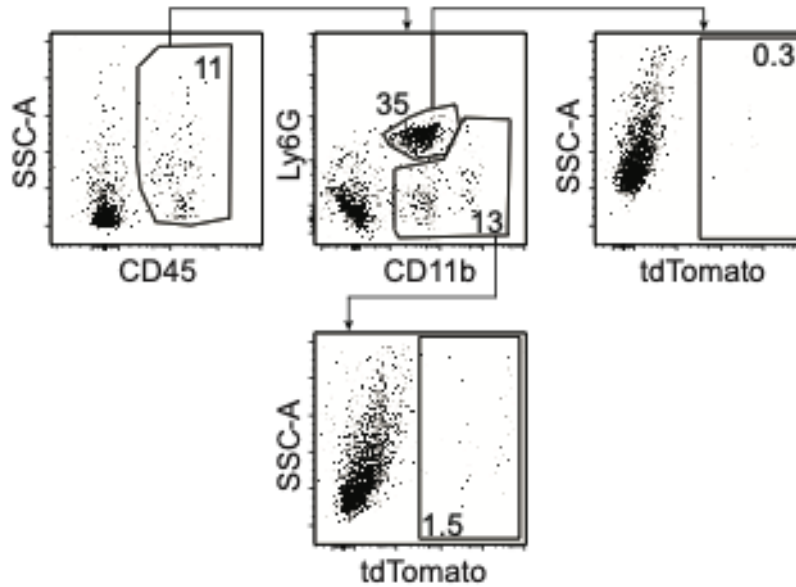
Fig. S4. Gating strategy for flow cytometry. Following removal of singlets and dead cells, cells were initially gated on CD45 expression. Based on expression of Ly6G and CD11b, cells were categorized as Neutrophils (CD45$^+$, CD11b$^+$, Ly6G$^+$) or as monocytes (CD45$^+$, CD11b$^+$, Ly6G$^-$)
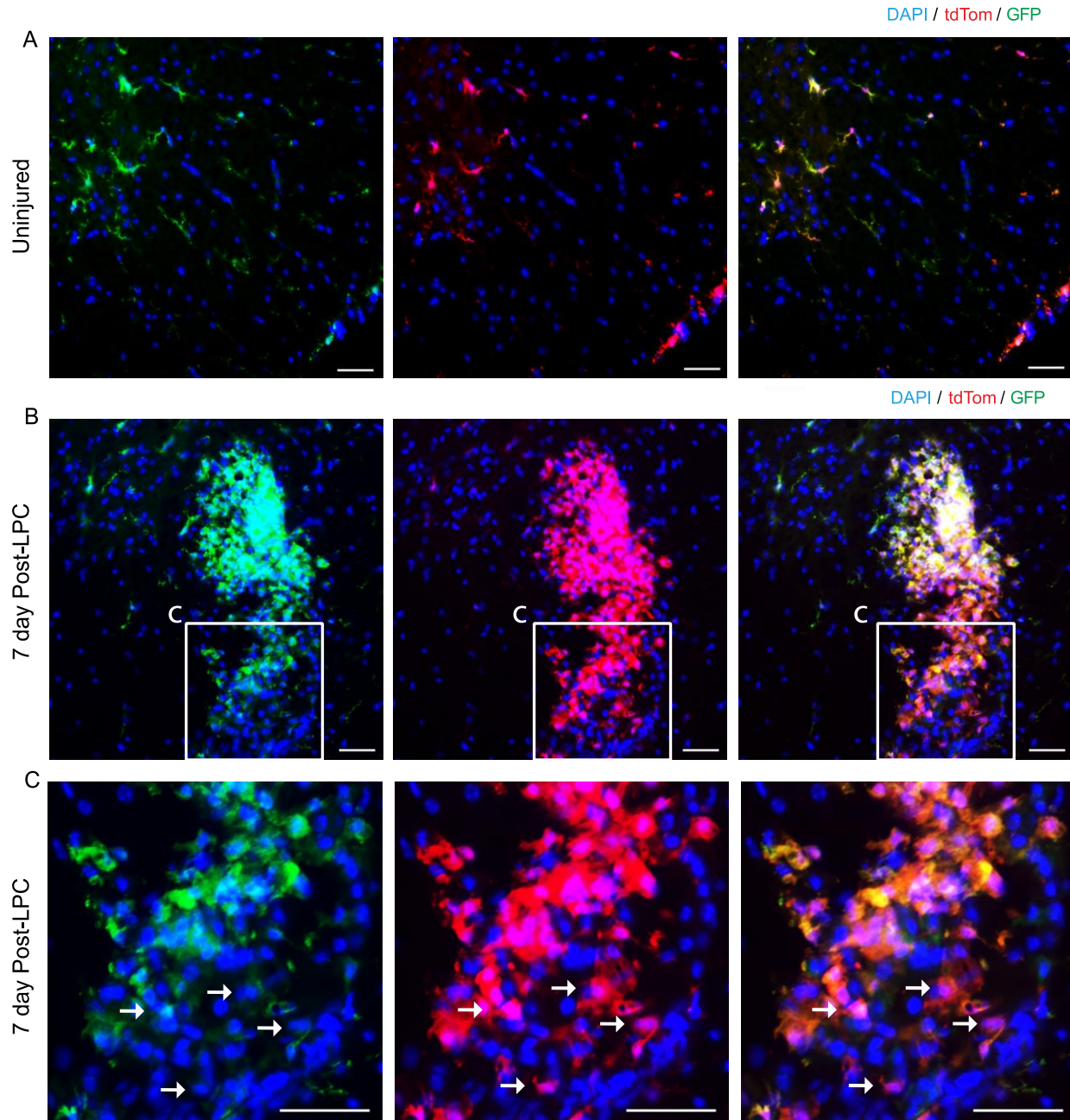
Fig. S5. Microglia express CX3CR1 and tdTomato. Under homeostatic conditions, microglia that are fate mapped (tdTom$^+$) also express CX3CR1 (EYFP$^+$) (**A**). After injury a population of fate mapped microglia (tdTom$^+$) express much reduced levels of CX3CR1 (EYFP) (**B**, **C**). Arrow label examples of tdTom$^+$EYFP^{low} cells. Scale bar, 20 μm.

A

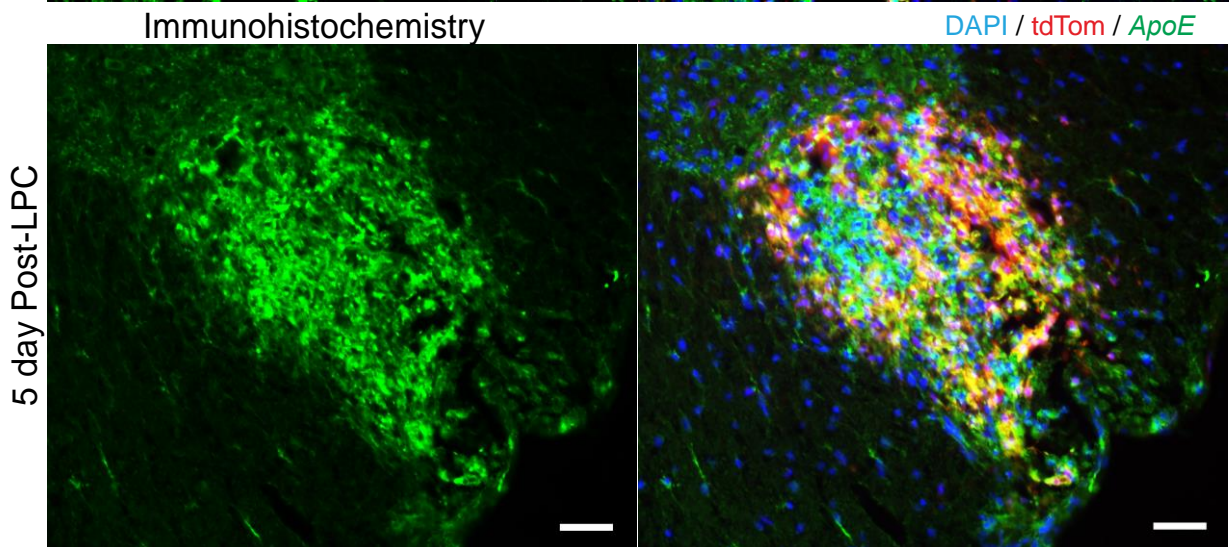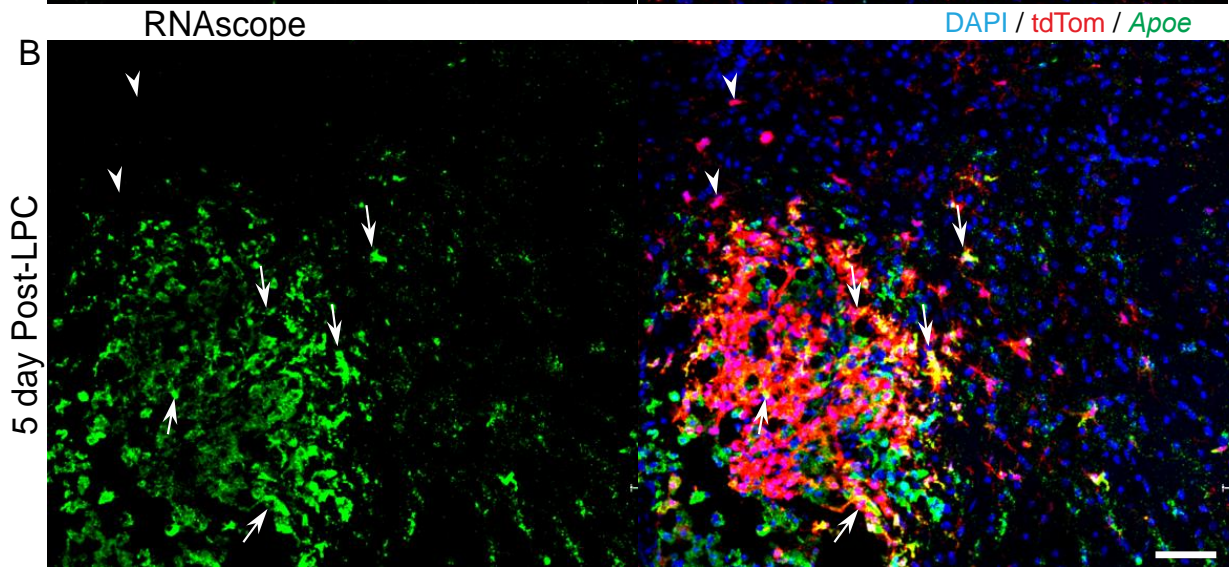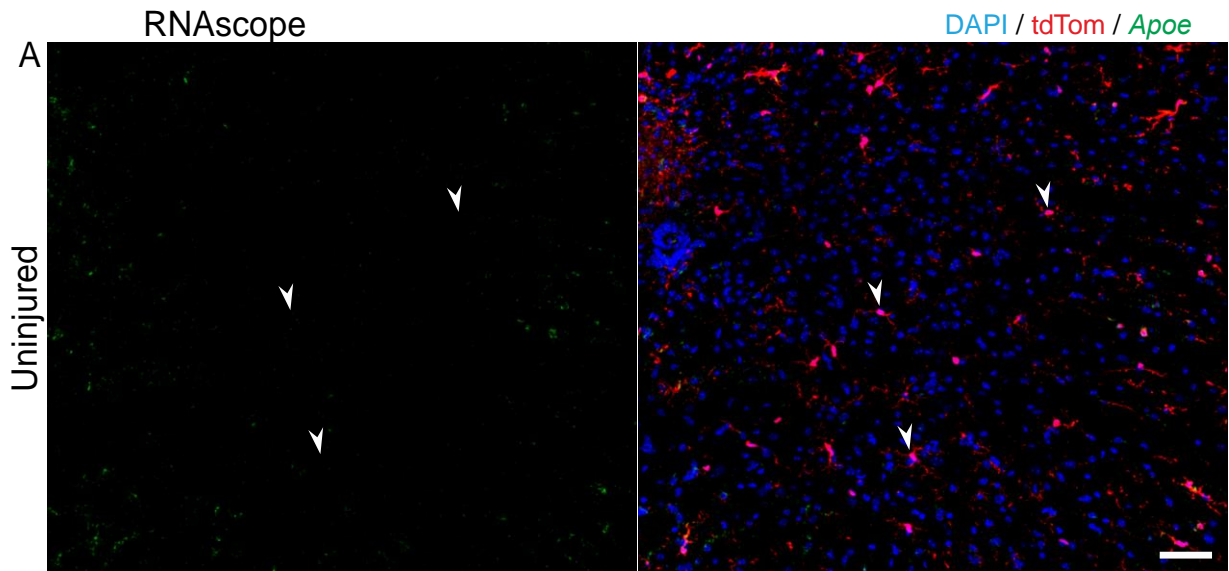|	Library 1	Library 2
Condition	Naïve	Lesioned
Estimated # of cells	705	580
Mean reads per cell	100,492	141,564
Median UMI counts per cell	2,982	4,382
Median genes per cell	1,273	1,560
Total # of reads	70,846,873	82,107,168
Confidently mapped reads	89.20%	89.30%
Q30 Bases in RNA Read	76.30%	74.50%
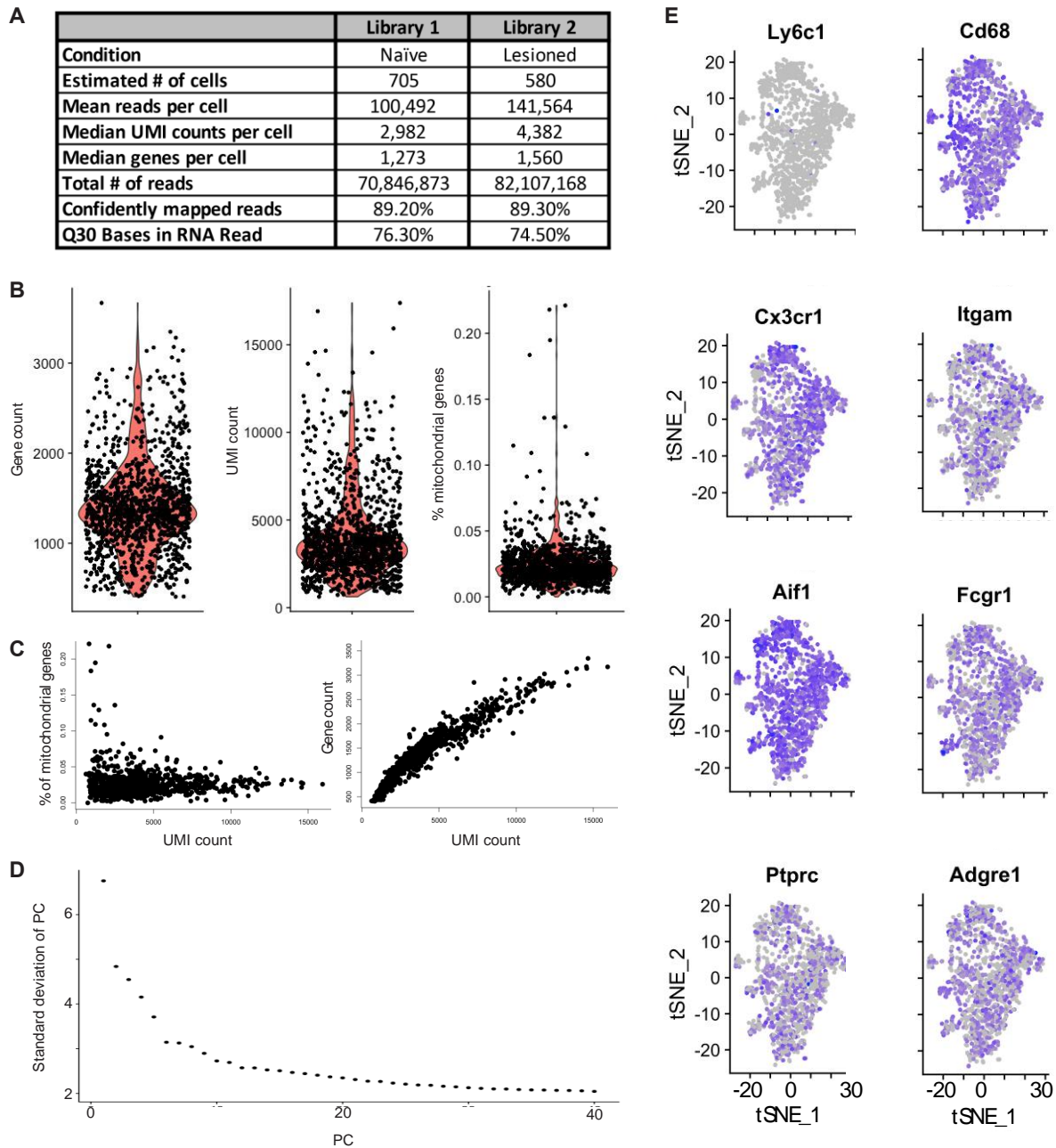
Fig. S6. RNA-seq experiment metrics and quality control. (**A**) Sequencing metrics for each individual library. (**B**) Gene counts, UMI and % mitochondria genes for each individual cell. (**C**) Correlation of UMI counts with % mitochondrial genes and total genes for each individual cell. (**D**) Elbow plot of the top 40 principle components. (**E**) Unsupervised graph-based clustering of selected genes in single-cell RNAseq dataset projected onto a tSNE plot. Ly6c1 (monocyte gene) would not be expected to be expressed by microglia whereas Cd68, Cx3cr1, Itgam, Aif1, Fcgr1, Ptprc and Adgre1 would.
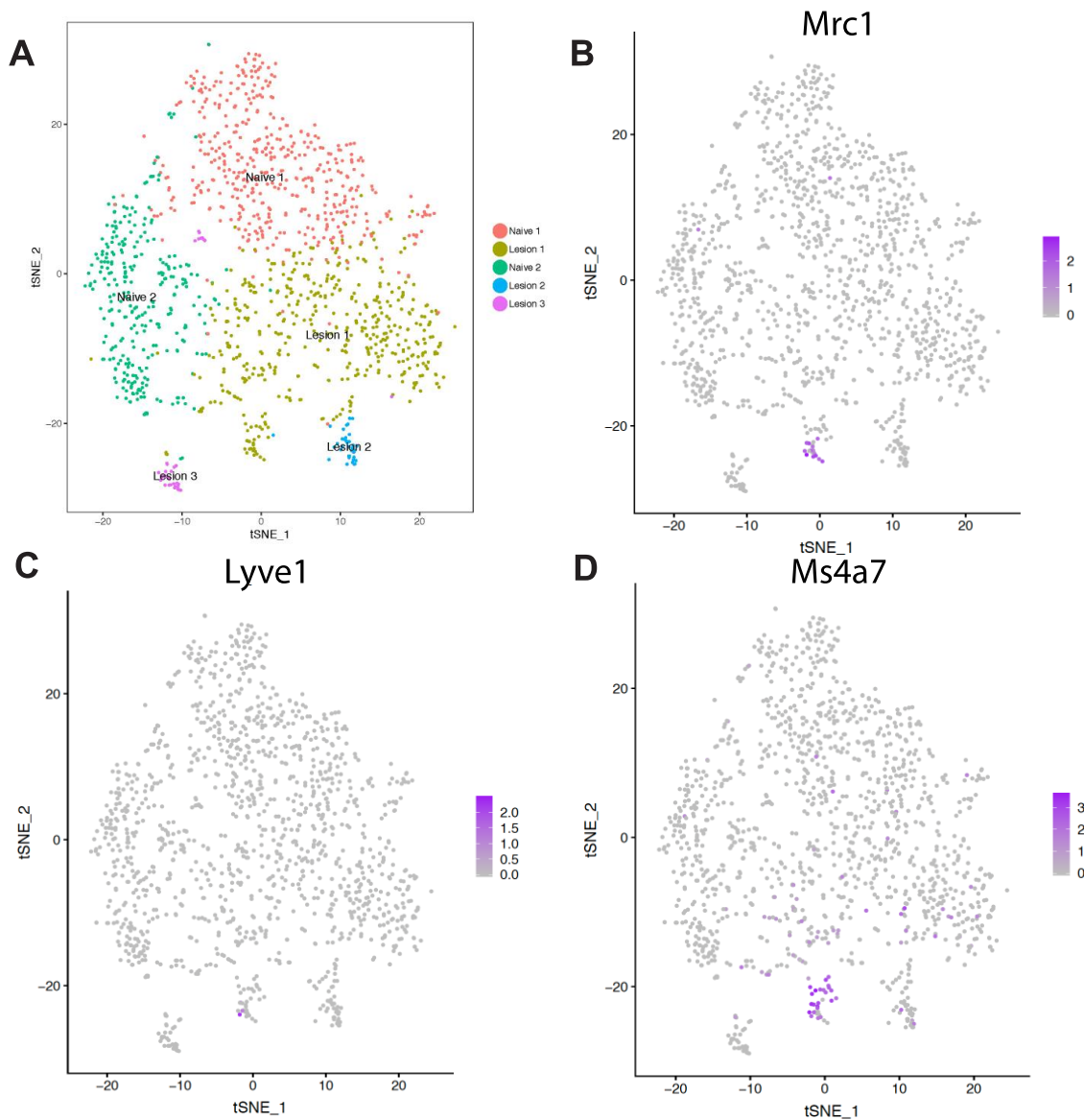
Fig. S7. Sparse CAM present following single-cell RNA sequencing of fate mapped cells (tdTom⁺). Unsupervised graph-based clustering of selected genes that are enriched for meningeal and perivascular macrophage markers (CAM) in single-cell RNAseq dataset projected onto a tSNE plot. tSNE plot of all tdTom cells with clustering patters (**A**). Expression of Mrc1 (**B**), Lyve1 (**C**) and Ms4a7 (**D**) within tSNE plots.

RNAscope   DAPI / tdTom / *Apoe*

Uninjured

RNAscope   DAPI / tdTom / *Apoe*

5 day Post-LPC

Immunohistochemistry   DAPI / tdTom / *ApoE*

5 day Post-LPC

Fig. S8. Activated microglia express ApoE. In the uninjured spinal cord, there was a paucity of *Apoe* mRNA expression (**A**) that was enriched in microglia 5 days following LPC-induced demyelination (**B**). Using immunohistochemistry, the protein expression of ApoE was confirmed in activated microglia. Scale bar, 10 µm (A, B) 20 µm (**C**).

M1 Phenotype

M2 Phenotype
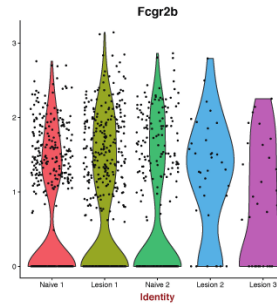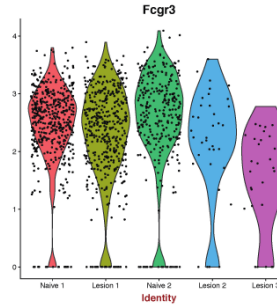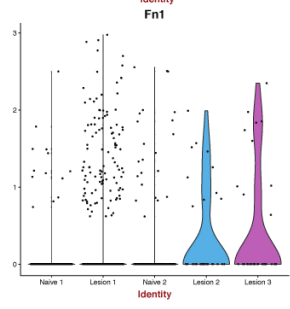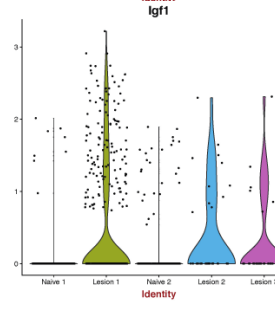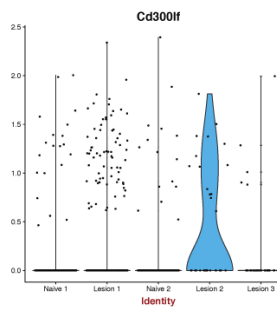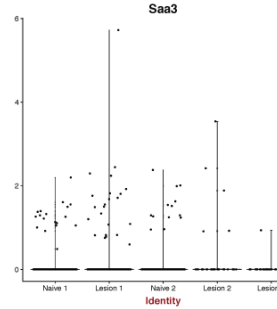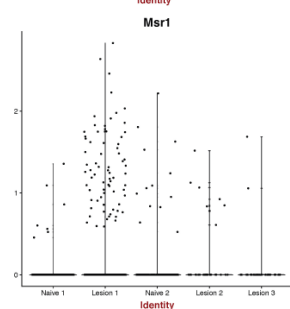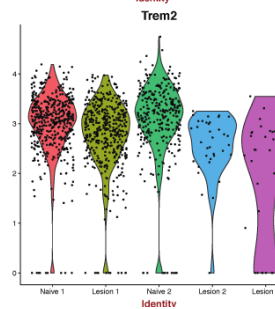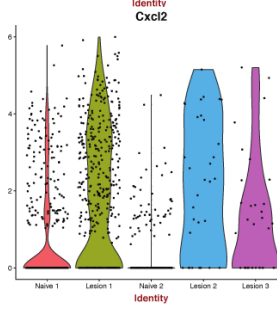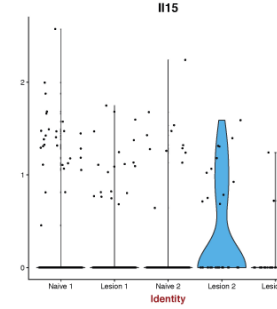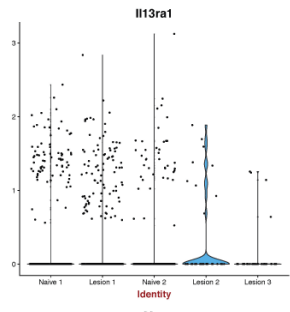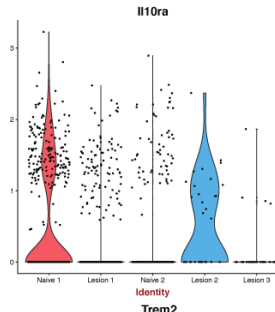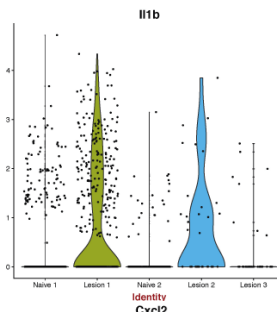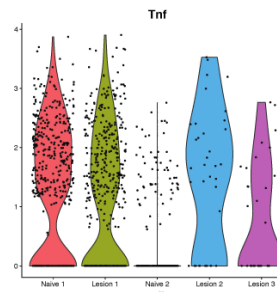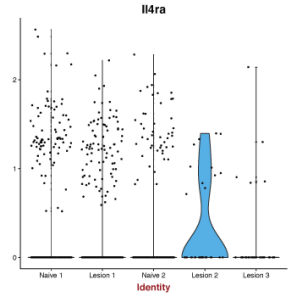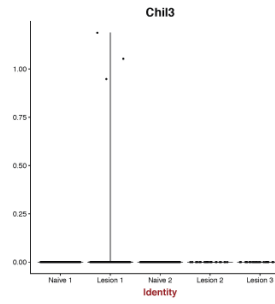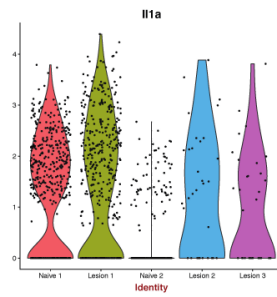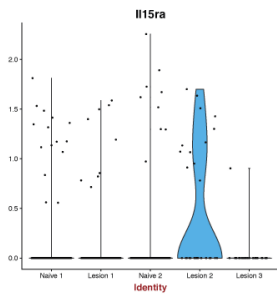
Fig. S9. M1 and M2 genes in scRNA sequencing dataset. Unsupervised graph-based clustering of selected genes in single-cell RNAseq dataset projected onto a tSNE plot. M1 markers include: Ccl5, Hspa1a, Ccl2, Ccl6, Ccl3, Cd86, Socs3, Tlr1. M2 markers include: Igf1, Egr2, Timp2, Ltc4s, Gas6, Ctsl, Stab1, Trem2 (based off of (*25, 26*))

A Cell fate 1 ... Cell fate 2

Cell Type

Genes (top to bottom): Cdkn1a, Ccnt1, Rrad, Pcf11, Sowahc, Rab20, Rel, Tgif1, Sdc4, Spag9, Ube2b, Klf6, Fosb, Mat2a, Tnpo3, Sde2, Nr4a1, Eif1a, Baiap2, Rbm39, Phlda1, Myd88, Dynll1, Gtf2b, Csrnp1, Skil, Kdm6b, Il1b, Tlr2, Ccl7, Cxcl2, Fcrls, Saa3, Apoc1, Irf7, Oasl2, Cd69, Ifitm3, Zbp1, Rtp4, Cd72, Bst2, Cst7, Wfdc17, Cybb, Ifitm2, Fxyd5, Cd9, Cd63, Ctsb, Bcl2a1a, Lmnb1, Gpr65, Ifi27l2a, Cd52, Csf1

Color scale: 2, 1, 0, -1, -2

B Aspect 1 2 3 4 5

C Aspect 2

Genes: Ifit1, Ifit3, Ifit3b, Usp18, Phf11d, Igtp, Pyhin1, Mnda, Irf7, Ifi47, Ifi205, Cmpk2, Gm4955, Iigp1, Ifit2, Rsad2, Mx1, Pydc4, Phf11a, Isg20

Aspect 3

Genes: Racgap1, Prc1, Cdca8, Pbk, Ube2c, Ccnb2, Birc5, Cdc20, Ccnb1, Cdca3, Cenpa, Plk1, Tpx2, Cdkn3, Rrm2, Top2a, Tk1, Nusap1, 2810417H1:, Spc25

Low — High
Expression magnitude

Low — High
Cell PCscore

Fig. S10. Distinct activated microglia subphenotypes. (**A**) Branched kinetic heatmap of significantly branch-dependent genes (BEAM analysis) revealed changes underlying transcriptional divergence between microglial Cell fate 1 and 2. *Cd69, Ifitm3/1, Cd9,* and *Cd72* etc exhibited branch-dependent enrichment towards Cell fate 1. (**B**) Pathway and gene set overdispersion (PAGODA analysis) highlighted gene sets exhibiting coordinated regulation in injury-activated microglia (cells are ordered based on coordinated expression of gene sets, and each cell is represented by either green, white or orange). Gene sets are summarized as 'aspects' with specified gene ontology (GO) annotations and novel gene sets that follow a pattern of coregulation. Aspect scores (Cell PC score) are oriented so that high values (dark orange) generally correspond to increased expression of associated gene sets. There was a defined subset of cells (orange) that had a transcriptional profile consistent with IFN activation (aspect 2) or mitosis (aspect 3). (**C**) Expression patterns of top-loading genes for Aspect 2 and 3. Aspect 2 was associated with GO terms linked with IFN stimulation, whereas Aspect 3 was enriched in genes associated with mitosis.

A 4 weeks post tamoxifen

PNS — TD Tomato/IBA1

B Recombination frequency in Resident macrophage (%tdTom+IBA1+/IBA1+)

4 Weeks post tamoxifen
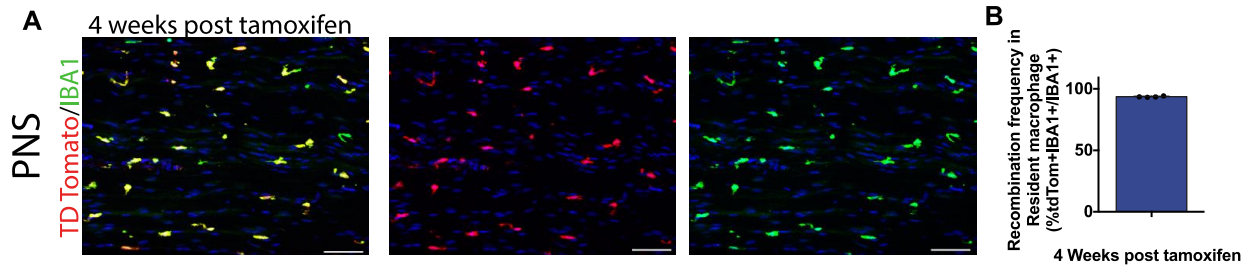
Fig. S11. Fate mapping as a tool to specifically label resident macrophage in sciatic nerve.
(**A, B**) Representative immunohistochemical images of the uninjured sciatic nerve demonstrated very high recombination efficiency at 4 weeks post tamoxifen (tdTom reporter, red; IBA1, green) (A). This observation was also reflected in quantification (B). n = 4 (B); Error bars indicate ± SEM. DPI = Days post LPC injection. Scale bar, 10 μm.
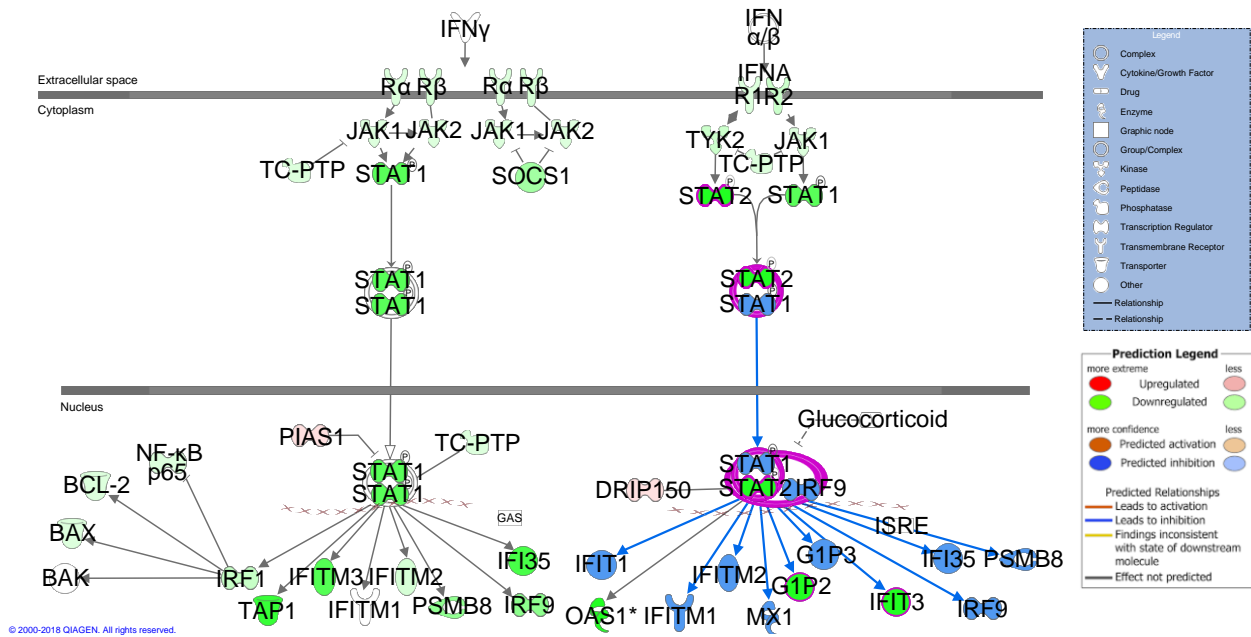

PNS   CNS
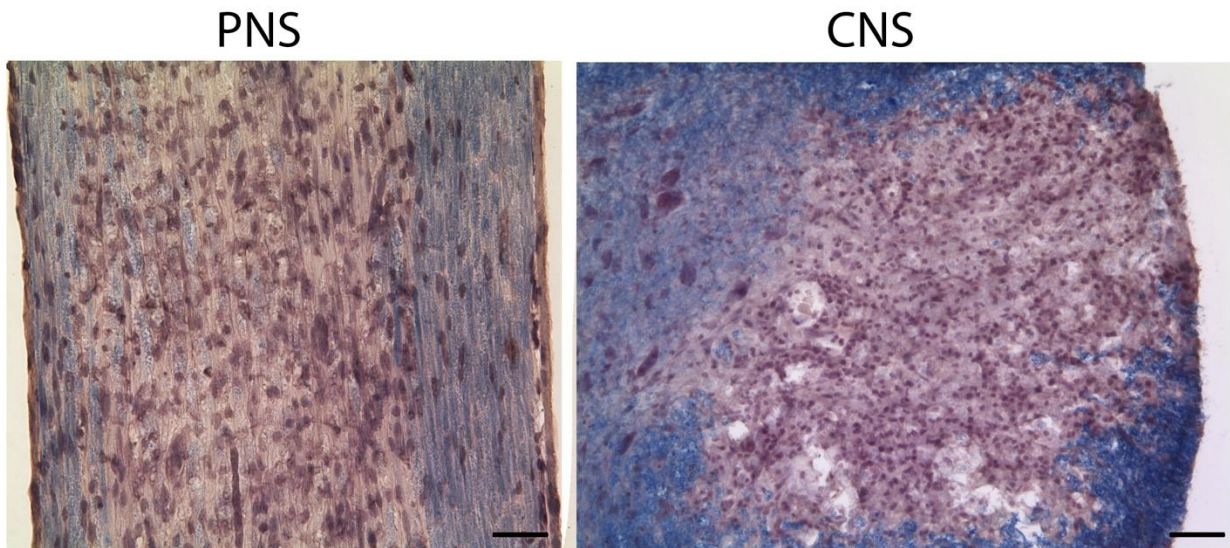
Fig. S12. CNS and PNS LPC injections. Comparison of CNS and PNS demyelination 7 days after demyelination using Eriochrome cyanine staining. Scale bar, 20 μm.
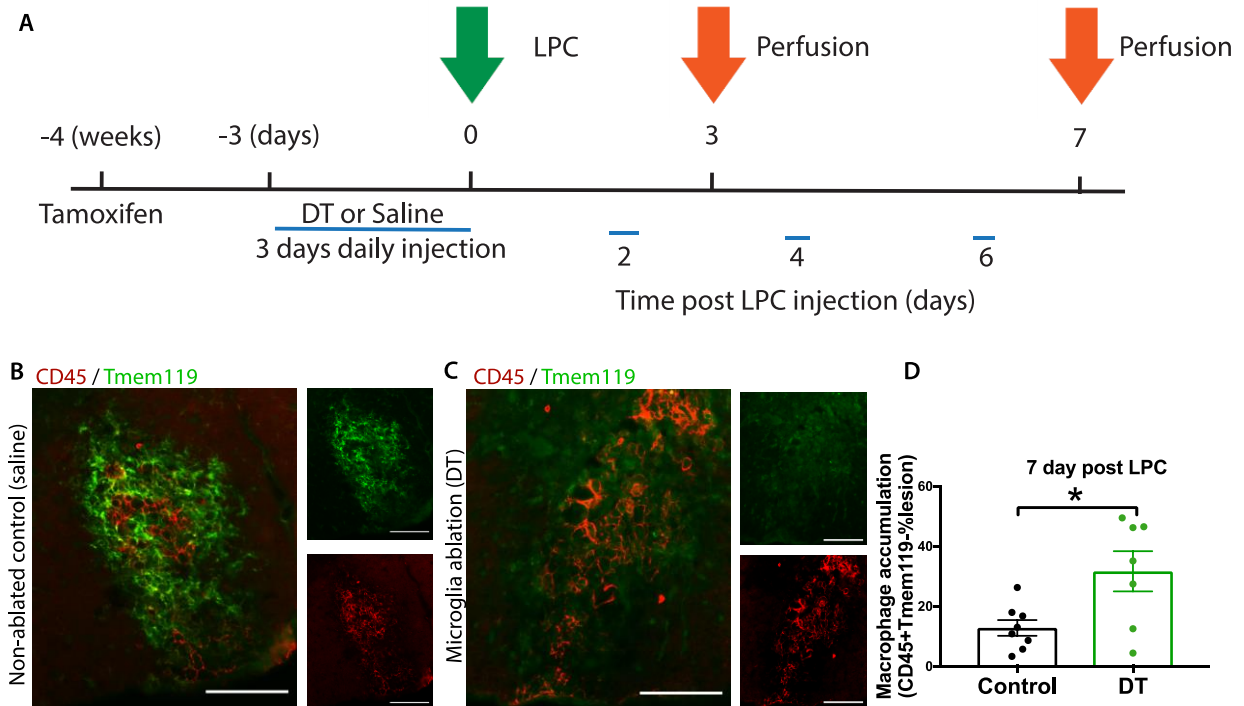
Fig. S13. Infiltrating macrophages expand in CNS when microglia/CAMs are ablated following LPC demyelination. Schematic of timeline for this experiment (**A**). Representative immunohistochemical images of the lesioned spinal cord in non-ablated (**B**) and DT ablated (**C**) mice demonstrating an expansion of CNS-infiltrating macrophages (CD45+ Tmem119-) following the ablation of microglia/ CAMs. This observation was reflected in quantification where the area (in pixels) occupied by macrophages was greater (**D**). Error bars indicate ± SEM. Scale bar, 20 μm.

Fig. S14. Cytosolic pattern recognition receptors reduced in the absence of microglia.
Ingenuity pathway analysis (IPA) of RNA sequencing data set comparing microglia ablation to
unablated demyelinated lesions. IPA demonstrates reduced levels of several cytosolic pattern
recognition signalling molecules. Genes downregulated are green, and upregulated in red.
Significant changes are demonstrated by purple.

Fig. S15. IFN type I and type II reduced in the absence of microglia. Ingenuity pathway analysis (IPA) of RNA sequencing data set comparing microglia ablation to unablated demyelinated lesions. IPA demonstrates reduced levels of type I and type II interferon (IFN) signalling. Genes downregulated are green, and upregulated in red. Significant changes are demonstrated by purple.